KONA Powder and Particle Journal No. 34 (2017) 248–257/Doi:10.14356/kona.2017014 Original Research Paper

Impact Dispersion Using 2D and 3D Composite Granular Packing †

Surajit Sen [1]*, T. R. Krishna Mohan [2] and Mukesh Tiwari [3]

[1] *Department of Physics, State University of New York, USA*
[2] *CSIR Centre for Mathematical Modelling and Computer Simulation (C-MMACS), India*
[3] *Group in Computational Science and High Performance Computing, DA-IICT, India*

Abstract

We present a study of efficient dispersion of an impact onto structured and potentially scalable granular beds. We use discrete element method based dynamical simulations of shock wave propagation and dispersion in 2D and 3D arrangements of granular spheres. The spheres are geometrically packed in a nested columnar structure, which leads to the severe attenuation and spreading of the incident energy within the structure. We further show that by incorporating inhomogeneity in material properties, or by introducing layers of a dissimilar material in the middle of the arrangement, impact mitigation can be enhanced significantly. Such an arrangement can therefore be useful in the design of effective impact decimation systems. Using a 2D arrangement we first show the basic idea behind impact dispersion in such an arrangement. With this understanding the system is scaled to 3D. The influence of the system size and material properties on the wave propagation within the packing is also presented.

Keywords: elastic grains, mass mismatch, impact dispersion, granular chain, solitary waves

Introduction

Impact dispersion is an important area of research with wide ranging combat related applications, applications in the study of earthquake resistant structures and so on. Impulse propagation in granular systems has been an important area of research for more than 30 years due to the unique properties observed as a result of the highly nonlinear contact law between the grains (Nesterenko V.F., 2001; Jaeger H.M. et al., 1996; Katsuragi H., 2016).

Starting with the pioneering work of Nesterenko (Nesterenko V.F., 1983), who showed the existence of solitary waves in a 1-dimensional arrangement of equal radius spheres, extensive work based on experiments (Coste C. et al., 1997), numerical simulations (Sinkovits R.S. and Sen S., 1995; Sen S. and Manciu M., 2001) and analytical methods (Mackay R.S., 1999; Lindenberg K. et al., 2011) have been performed for one dimensional chains (see e.g., Sen S. et al., 2008 for an exhaustive review). These studies have been instrumental in the design of novel granular materials with widespread applications. It is now well understood that introducing a mass mismatch in these one dimensional granular systems, either by changing the size of the spheres such as in tapered (Doney R. and Sen S., 2005; Nakagawa M. et al., 2003; Melo F. et al., 2006) and decorated chains (see e.g., Doney R. and Sen S., 2006;, Machado L.P. et al., 2014), or by changing of the material properties by introducing spheres of different materials (Hong J. and Xu A., 2002; Hong J., 2005; Nesterenko V.F. et al., 2005; Daraio C. et al., 2006; Wang P.J. et al., 2007; Fraternali F. et al., 2010) leads to the rapid disintegration of the moving solitary wave, which would be of importance in designing materials for impact decimation.

Impact response of 2-dimensional granular systems has been studied extensively through experiments and numerical simulations of photoelastic disks by Shukla et al. (Rossmanith H.P. and Shukla A., 1982; Zhu Y. et al., 1996; Sadd M.H. et al., 1993). More recently, Nishida et al. have studied projectile impact and wave propagation in two dimensional granular arrangement, including the effect of dissimilar materials (Nishida M. et al., 2001; Tanaka K. et al., 2002; Nishida M. and Tanaka Y., 2010). Leonard et al. through a series of works have systematically studied the role of the intruders and disorder on two dimensional square and hexagonal arrangements of granular systems (Leonard A. and Daraio C., 2012; Leonard A.

† Received 18 April 2016; Accepted 18 June 2016
J-STAGE Advance Publication online 30 July 2016
[1] Buffalo, New York 14260-1500, USA
[2] Bangalore, Karnataka 560037, India
[3] Gandhinagar, Gujarat 382007, India
* Corresponding author: Surajit Sen;
E-mail: sen@buffalo.edu
TEL: +1-716-907-4961 FAX: +1-716-645-2507

et al., 2012, 2013, 2014). The role of the intruders and the different modes of propagation have been studied numerically by Awasthi et al. (Awasthi A.P. et al., 2012; Awasthi A.P. et al., 2015). The force propagation speed and effects of dissipation has also been analyzed (Abd-Elhady M.S. et al., 2010; Pal R.K. et al., 2013; Burgoyne H.A. and Daraio C., 2015). The 3-dimensional studies on monodispersed sphere arrangements have explored wave propagation (Manjunath M. et al., 2014), effect of impact conditions on the rebound velocity of the incident projectile (Nishida M. et al., 2004) and the impact response of heterogeneous granular systems (Burgoyne H.A. et al., 2015).

2. Model and numerical method

2.1 Quasi-2D bed

Fig. 1 shows the schematic of a recently proposed two dimensional granular arrangement (Tiwari M. et al., 2016) for impact decimation, wherein, spherical granular particles are assembled in a block-type arrangement. The spheres in a block are of equal masses and have the same material properties. The radius of the spheres in any block is, however, twice that of spheres in the block immediately below it. It should be emphasized that the geometries of the systems discussed here all require a factor of two reduction in sphere radius at each interface. Within each block we have rectangular arrangement of monodispersed spheres, and the blocks are placed in such a way that at the interface the sphere with larger radius is placed symmetrically above the two smaller spheres in the block below. This is also shown in the enlarged view in **Fig. 1**.

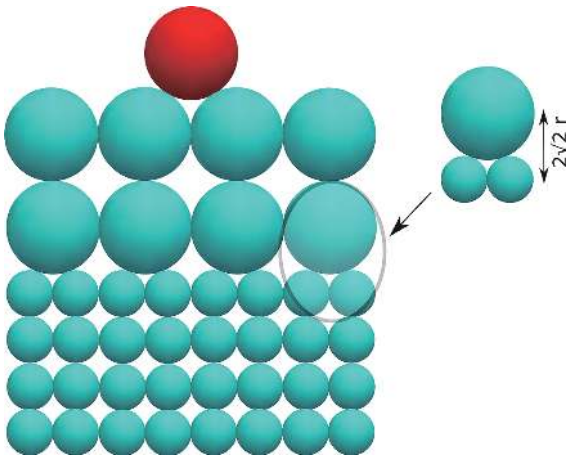

Fig. 1 Schematic of a part of the two dimensional granular arrangement with two blocks. The side walls are to be regarded as infinitely far away. The lower block is made up of spheres of radius r and the top block has spheres of radius $2r$.

The spheres are initially assumed to be in contact with no precompression, and interact elastically upon compression. The normal and tangential components of the force depend on the overlap and can be written as,

$$F_n = k_n \delta_n, \tag{1}$$

$$F_t = k_t \delta_t, \tag{2}$$

δ_n and δ_t are the normal and tangential overlap, respectively. For two spheres with separation r and radii R_1 and R_2 the normal overlap $\delta_n = R_1 + R_2 - r$ and the contact force is nonzero only when $\delta_n > 0$. The tangential overlap δ_t is the relative tangential displacement between the two spheres for the entire contact duration and the tangential force is limited by the coulomb criterion $F_t = \min(F_t, \mu F_n)$. We use the nonlinear Hertz contact interaction for describing the normal force in our simulations (Hertz H., 1881). The spring constants k_n and k_t therefore depend on the normal overlap in addition to the material parameters, $k_n = \frac{4}{3} Y^* \sqrt{R^* \delta_n}$ and $k_t = 8G^* \sqrt{R^* \delta_n}$. For spheres with the same Young's modulus Y and Poisson's ratio v the effective Young's modulus $Y^* = \frac{Y}{2(1-v^2)}$ and the effective shear modulus $G^* = \frac{Y}{4(1-2v)(1+v)}$. R^* is the effective radius and equals $\frac{R_1 R_2}{R_1 + R_2}$. For numerical simulation of the system we use the open source DEM package LIGGGHTS (Cundall P.A. and Strack O.D.L., 1979; Kloss C. et al., 2012; Plimpton S.J., 1995). We do not include gravity in our numerical simulations. The effect due to gravity would become significant for a large number of particles and weak impulse. For strong impulse the disturbance would still travel as solitary waves (Hong J. and Xu A., 2001). No dissipation of any form is taken into account, however, we do consider the effect of static friction on the distribution of energy. Incorporating dissipation would undoubtedly improve the impact decimation capabilities of the systems we study. However, ignoring dissipation in the following calculations help us set an upper bound on how much energy can be dispersed by the systems we examine.

Since the spheres interact only if they are in contact, the energy due to the impact by the striker travels along

Table 1 Densities, Young's moduli and Poisson's ratio of different materials used in numerical simulations.

	ρ (kg/m^3)	Y (Pa)	v
Steel	7833	193×10^9	0.3
Teflon	2170	1.46×10^9	0.46

the chains of spheres in line with the contact point of the striker. We assume that the striker impact is in between two of the spheres in the upper most layer. For simplicity, we also assume that the striker is of the same mass and material as the spheres in the top block. The energy in the top block therefore travels sideways in the top layers, and downwards along two vertical chains. For a single block system with a square arrangement of purely elastic spheres it has been observed that around 71.5 % of the energy propagates downwards whereas the sideward propagation is around 24.5 % (Leonard A. et al., 2013). Our numerical simulations were consistent with these observations. The sideward propagation was observed to be significantly suppressed if static friction was included in our numerical simulations. We therefore, focus only on the downward propagating part. We will briefly comment in the following on what happens when the mass of the striker is increased or decreased.

2.2 Impact decimation by a quasi 2D bed

The system in the absence of multiple blocks is only one dimensional. Presence of multiple blocks makes it quasi two dimensional, since due to the proposed arrangement of spheres at the interface of two blocks, the energy from any excited larger spheres gets transmitted to two smaller spheres that are in contact with it in the block below. The spatial extent, however, remains the same due to the smaller radii of the spheres across the interface.

In **Fig. 2** we show the propagation of kinetic energy in a two block system at different time instants for particles made from steel in both the blocks. The energy as expected propagates in a localized manner in the top block (**Fig. 2(a)**) along two chains. As this energy crosses the interface and moves to the block with lighter spheres it tends to spread out in its direction of propagation (see **Fig. 2(b)**), and after this transient phase it is seen to move as well separated discrete packets or solitary wave trains with much smaller energies in each pulse. The energy in each pulse of the wave train depends on the difference of the masses of the two spheres (Job S. et al., 2007). It is worth noting that impact of a striker which is more massive than the masses of the grains in the bed leads to the formation of solitary wave trains in the first block itself. No such trains form when a striker of lighter mass impacts on to the bed.

Presence of more blocks would lead to further frag-

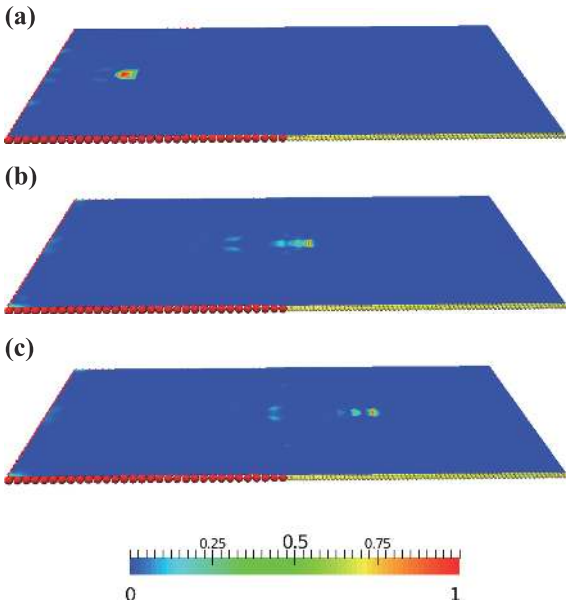

Fig. 2 Surface plots of the kinetic energy propagation in a two block system for three different time instants: **(a)** the energy is in the upper block **(b)** at the interface and **(c)** the energy is in the lower block. The kinetic energy is normalized to its maximum value for that time instant. The spheres in upper and lower blocks are shown in red and yellow respectively.

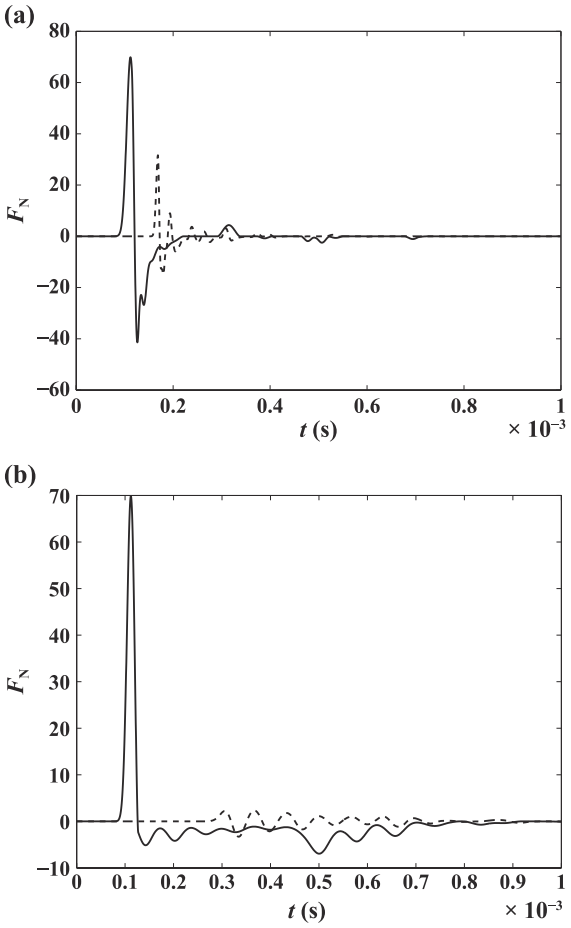

Fig. 3 Normal force experienced by the larger sphere at the interface of a 3 block system made of **(a)** steel grains and **(b)** block made from Teflon spheres sandwiched between two blocks made of steel spheres. The solid line is for a sphere at the top interface while dashed line is for the bottom interface.

mentation of these pulses at each interface. An effective impact decimation system can be constructed by having a multiple block arrangement. We consider two such arrangements each consisting of three blocks. In the first arrangement all the blocks are made from steel spheres, whereas, in the second arrangement a block made from lighter material such as teflon is sandwiched between two blocks made from steel spheres. The masses differ by a factor of 8 at each interface in the first arrangement whereas in the second arrangement they differ by a factor of 29.5 and 2.2 at the steel-teflon and teflon-steel interface respectively. Even though the numbers of interfaces are the same the difference in mass mismatch is seen to affect the impact decimation ability significantly. The normal force experienced by the larger sphere at the interface for the two arrangements are shown in **Figs. 3(a)** and **(b)** respectively. At the first interface (solid line in **Fig. 3**) sustained small amplitude oscillations are observed in the second arrangement. For larger mass mismatch values the solitary wave in the top block splits into more number of pulses with smaller amplitude when it moves to the second block. Each of these pulses split further at the second interface since they still move from a heavier side to a lighter side. This results in the further decimation of each pulse. This is shown through the dashed line in **Fig. 3**.

2.3 Hard sphere collision approximation (energy transmission in a multi-block system)

In the previous section we observed that a multi-block system results in significant decimation of the impact energy. Using a hard sphere approximation we provide an estimate of the output kinetic energy of the system. We consider a simplified picture in which we first estimate the transmitted energy in a general three sphere collision with the arrangement shown in **Fig. 4**. This is similar to the arrangement of the spheres at the interface of $i-1^{\text{th}}$ and i^{th} block. We ignore any horizontal momentum transfer to these spheres from the adjacent spheres. Using conservation of energy and momentum we can write for the momentum of the spheres

$$p_{i,1}^{y} = p_{i,2}^{y},$$

$$p_{i-1}^{x}(0) = p_{i-1}^{x}(f) + 2p_{i,1}\cos\theta,$$

$$p_{i-1}^{2}(0) = p_{i-1}^{2}(f) + 2\epsilon p_{i,1}^{2} \tag{3}$$

where $p_i^{x,y}$ represents the x, y component of the momentum of the spheres in the i^{th} block, $\epsilon = \dfrac{m_{i-1}}{m_i}$ is the ratio of the masses of the sphere in the two blocks, and for the arrangement considered at the interface, $\cos\theta = \dfrac{2\sqrt{2}}{3}$. Due to the symmetry in the collision, the two smaller spheres move with equal momentum ($p_{i,1}^{x} = p_{i,2}^{x}$) after impact. The final momentum of the spheres from **Eq. (3)** is

$$\frac{p_{i,1}^{x}}{p_{i-1}(0)} = \frac{2\cos^2\theta}{\epsilon + 2\cos^2\theta}, \tag{4}$$

$$\frac{p_{i-1}}{p_{i-1}(0)} = \frac{\epsilon - 2\cos^2\theta}{\epsilon + 2\cos^2\theta}. \tag{5}$$

If $\epsilon - 2\cos^2\theta > 0$ ($\epsilon > 16/9$) from **Eq. (5)**, the top sphere would continue to move in its original direction. This leads to multiple collisions at the interface in the proposed system. Each collision leads to the generation of a solitary wave. From **Eq. (4)**, the momentum transfer is inversely related to the mass ratio. Therefore larger mass mismatch would result in a smaller momentum or energy transmission at each collision. It has been shown that the total energy carried by the solitary wave is $E = P^2/2m_{\text{eff}}$ where the effective mass of the solitary wave is $m_{\text{eff}} \approx \Omega m$. The value of Ω is approximately 1.4 (Job S. et al., 2007; Tichler A.M., et al., 2013). We further assume that the energy and momentum transfer between subsequent blocks is through the collision between solitary waves, and that the individual pulses in the solitary wave train are separated significantly. To calculate the output energy of the system we therefore only need to consider the leading solitary wave pulse in each block. Under these assumptions the complete energy transfer can be thought to occur as discrete events. At the initial time, the impact by the striker results in the generation of a solitary wave in the top block. Therefore, the collision process here is between a particle and solitary wave treated as a quasiparticle. At the second interface, the collision is between the two leading solitary waves on either side of the interface. Finally, in the lowest block the solitary wave transfers its

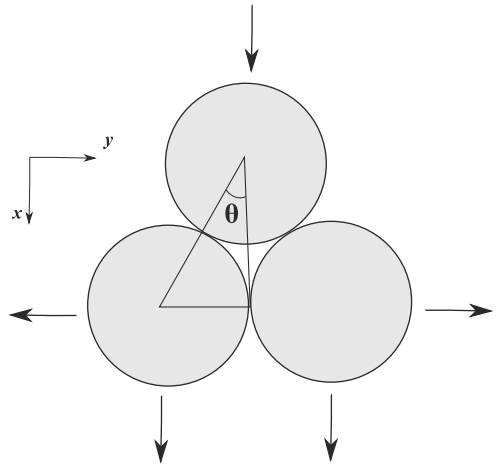

Fig. 4 Schematic for the sphere arrangement at the interface. The vertical downward direction is the x-direction and horizontal direction is the y-direction.

complete energy to the last particle which is taken to be the output energy of the system. The ratio of the momentum of the last particle in an n block system and the striker can then be written as:

$$\frac{p_{n,\mathrm{L}}}{p_{\mathrm{st}}(0)} = \left(\frac{p_{n,\mathrm{L}}}{p_{\mathrm{sw},n}}\right) \times \left(\frac{p_{\mathrm{sw},n}}{p_{\mathrm{sw},n-1}}\right)\left(\frac{p_{\mathrm{sw},n-1}}{p_{\mathrm{sw},n-2}}\right)\ldots\left(\frac{p_{2,1}}{p_{\mathrm{sw},1}}\right)\left(\frac{p_{\mathrm{sw},1}}{p_{\mathrm{st}}(0)}\right). \quad (6)$$

$p_{n,\mathrm{L}}$ is the momentum of the last particle in the n^{th} block, $p_{\mathrm{sw},i}$ is the momentum of the leading solitary wave pulse in the i^{th} block and $p_{\mathrm{st}}(0)$ is the initial momentum of the striker, $\frac{p_{n,L}}{p_{\mathrm{sw},n}} = \frac{2}{\Omega+1}$, and, $\frac{p_{\mathrm{sw},1}}{p_{\mathrm{st}}(0)} = \frac{2\Omega\cos^2\theta_1}{1+2\Omega\cos^2\theta_1}$. θ_1 is the angle that the striker makes with the two spheres ($\cos\theta_1 = 1/\sqrt{3}$). If the spheres are made from the same material **Eq. (6)** can be simplified and written as:

$$\frac{p_{n,\mathrm{L}}}{p_{\mathrm{st}}(0)} = \left(\frac{p_{n,\mathrm{L}}}{p_{\mathrm{sw},n}}\right)\left(\frac{2\cos^2\theta}{\epsilon+2\cos^2\theta}\right)^{n-1}\left(\frac{p_{\mathrm{sw},1}}{p_{\mathrm{st}}(0)}\right). \quad (7)$$

For alternating blocks of hard and soft material, such as steel-teflon-steel-teflon we can obtain a similar expression,

$$\frac{p_{n,\mathrm{L}}}{p_{\mathrm{st}}(0)} = \left(\frac{p_{n,\mathrm{L}}}{p_{\mathrm{sw},n}}\right)\left(\frac{2\cos^2\theta}{\epsilon_{\mathrm{st,tf}}+2\cos^2\theta}\right)^{p} \times \left(\frac{2\cos^2\theta}{\epsilon_{\mathrm{tf,st}}+2\cos^2\theta}\right)^{q}\left(\frac{p_{\mathrm{sw},1}}{p_{\mathrm{st}}(0)}\right), \quad (8)$$

where, $\epsilon_{\mathrm{st,tf}} = \frac{m_{\mathrm{st}}}{m_{\mathrm{tf}}}$. The powers p and q equals, respectively, $n/2$ and $\frac{n}{2}-1$ if n is even, while, if n is odd they are both equal to $(n-1)/2$. A better approximation to the energy transmission is obtained if we assume that within each block the solitary wave transfers its momentum and energy to the last particle of the block. Each collision of this last particle with the top particle in the next block leads to the generation of a solitary wave. Therefore at each interface the collision is between the particle on one side and the leading edge of the solitary wave treated as a quasiparticle on the other side. Under this assumption we obtain for spheres of the same material

$$\frac{p_{n,\mathrm{L}}}{p_{\mathrm{st}}(0)} = \left(\frac{p_{n,\mathrm{L}}}{p_{\mathrm{sw},n}}\right)\left(\frac{2}{\Omega+1}\right)^{n-1} \times \left(\frac{2\Omega\cos^2\theta}{\epsilon+2\Omega\cos^2\theta}\right)^{n-1}\left(\frac{p_{\mathrm{sw},1}}{p_{\mathrm{st}}(0)}\right), \quad (9)$$

and, for alternate blocks of steel and teflon

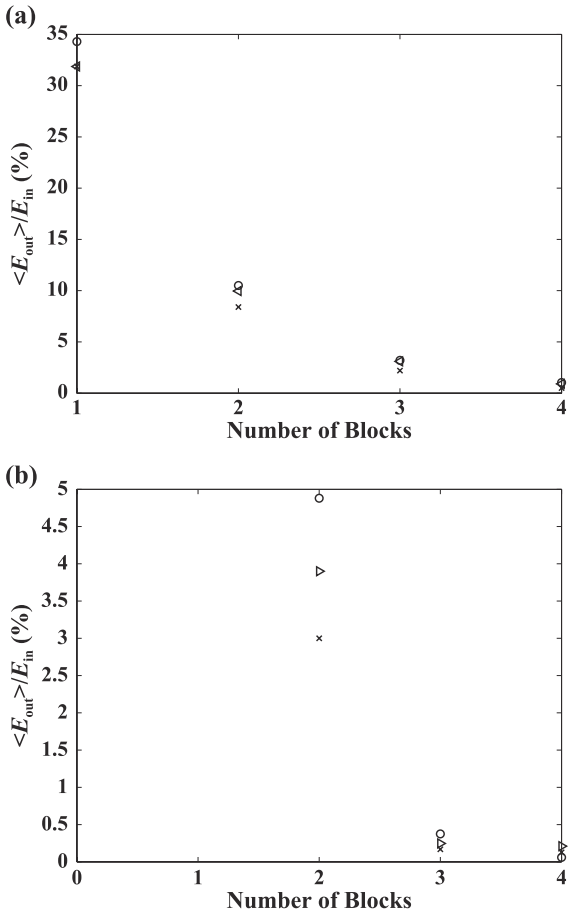

Fig. 5 Average Kinetic energy for 1–4 block system with **(a)** each block made of steel spheres and **(b)** alternate blocks with steel and Teflon spheres. The circles are obtained through numerical simulation whereas (×) is obtained from **Eqs. (7)** and **(8)**, and, (△) is obtained from **Eqs. (9)** and **(10)**.

$$\frac{p_{n,\mathrm{L}}}{p_{\mathrm{st}}(0)} = \left(\frac{p_{n,\mathrm{L}}}{p_{\mathrm{sw},n}}\right)\left(\frac{2}{\Omega+1}\right)^{n-1} \times \left(\frac{2\Omega\cos^2\theta}{\epsilon_{\mathrm{st,tf}}+2\Omega\cos^2\theta}\right)^{p}\left(\frac{2\Omega\cos^2\theta}{\epsilon_{\mathrm{tf,st}}+2\Omega\cos^2\theta}\right)^{q}\left(\frac{p_{\mathrm{sw},1}}{p_{\mathrm{st}}(0)}\right). \quad (10)$$

The average kinetic energy transmitted $\left(\frac{m_{\mathrm{st}}}{m_n}\right)\left(\frac{\langle p_{n,\mathrm{L}}^2\rangle}{p_{\mathrm{st}}^2(0)}\right)$ is shown in **Fig. 5** for multiple blocks (1–4 block system), m_n is the mass of the sphere in the n^{th} block. The average here is over the energies of all the excited spheres in the bottom layer of the last block. For comparison, in **Fig. 5** we only show the kinetic energy when the leading pulse reaches the last layer. In both the cases, **Eqs. (9)** and **(10)** are able to provide a better estimate, however, for dissimilar materials the fit is only qualitative. In **Fig. 5**, the energy shown is the leading energy of the pulse reaching the last sphere. The energy with which the last particle ejects is slightly larger than this value. Nevertheless, this difference is insignificant. More importantly, even with three blocks the average output energy is only around 0.4 % of

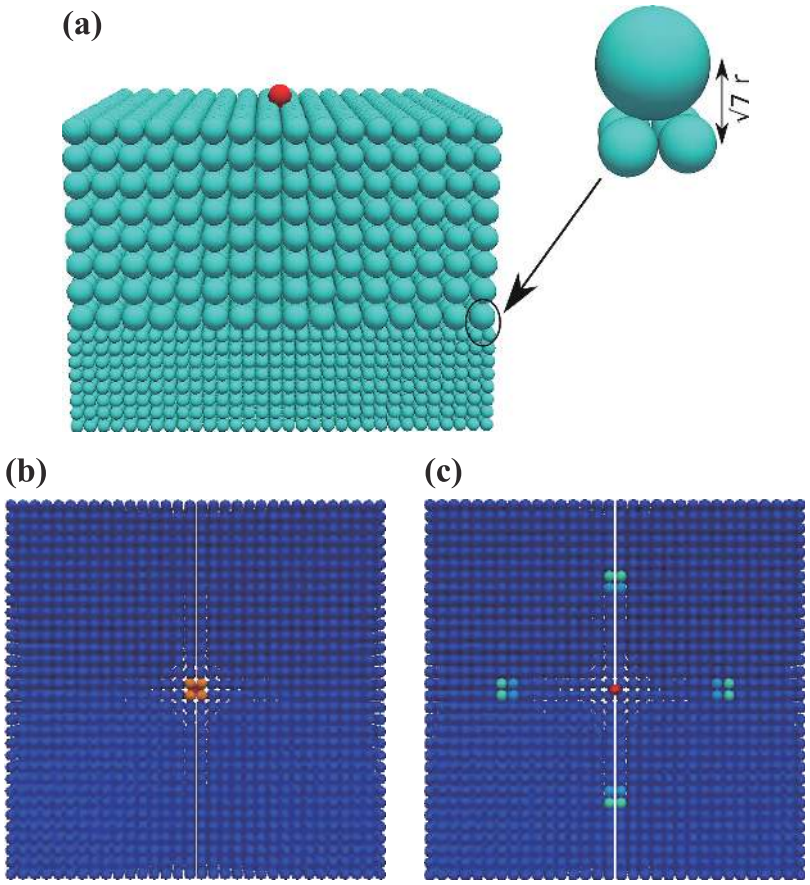

Fig. 6 (Top) Schematic of the 3-dimensional system with two blocks. (Bottom) Propagation of energy in a single block system (Left) vertically downward and (Right) sideward.

the impact energy. This energy does not show any significant dependence on the size of the system.

3. Impact decimation by a 3D bed

The advantage of the proposed system in two dimensions is that it can be easily extended to three dimensions. In **Fig. 6** (top) we show a typical three dimensional system with two blocks. As is evident from the enlarged view of the sphere arrangement at the interface, the larger sphere is in contact with four spheres in the layer below. The centers of the spheres form a pyramid like structure, with the base made from the plane connecting the centers of the four small spheres and the larger sphere is centered at the top of the pyramid at a vertical distance of $\sqrt{7}$ from the base. This pyramid structure forms the basis of energy partitioning at each interface. Each excited sphere transmits its energy to four spheres in the downward direction. The energy propagation for a single excited sphere is therefore through four chains vertically downward and eight chains in the lateral direction (see **Fig. 6** (bottom)). The process gets repeated at each interface and the energy is transferred to four times the number of excited spheres in the upper block. We show this energy partitioning for a completely elastic 1-block system in **Fig. 7**. What is notable is that the net energy transmission in the horizontal and vertical directions is almost the same. The rebound energy of the striker is higher (approx 12.5 %) than that of the two dimensional system (approx 4 %). Before energy exits from the system the distribution between potential and kinetic energy follows the virial theorem. Since the energy partitioning along the two directions are the same we also look at the effect of static friction on the distribution of energy. As shown in the bottom plot in **Fig. 7(b)** static friction does have the effect of reducing the sideward energy propagation. For higher values of static friction and when the boundaries are sufficiently far away or the side walls are made to be energy absorptive, these multi-block systems may be useful in many impact dispersion applications. The system properties would not change if the grain sizes were smaller as long as the elastic properties of the spheres were unaffected. Realistically this means the systems envisioned here could well be realized possibly even in the micron scale. In a regularly arranged closed packing we do not expect much rotational motion to occur, and therefore it is possible that energy propagation in the sideward direction

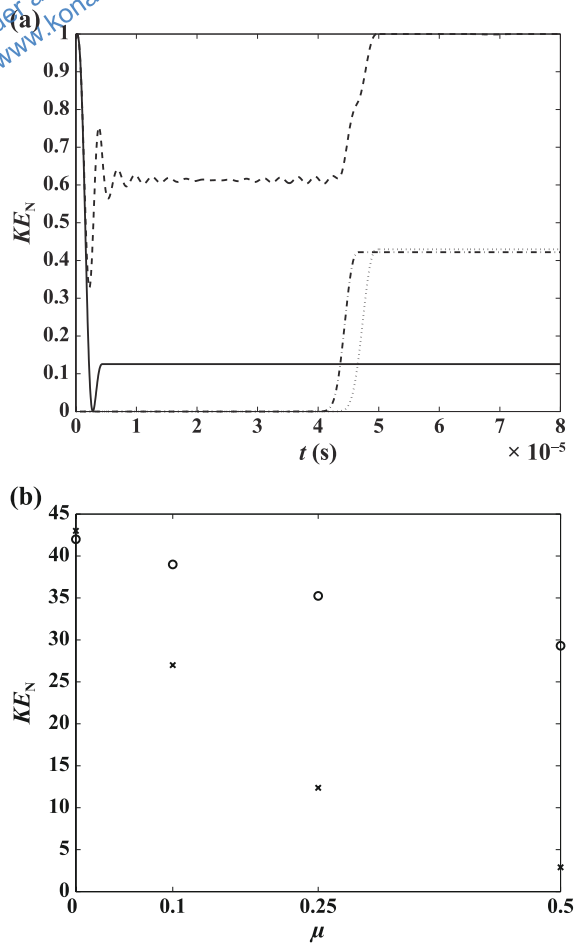

Fig. 7 **(a)** Partitioning of the normalized energy in a 1 block system, between the striker (solid line), four particles in the bottom layer (dashed-dotted line), and eight particles in the top layer (dashed-line). The dashed line shows the overall kinetic energy of the entire system (bed and striker). **(b)** Variation of normal (○) and sideward (×) transmission of total kinetic energy propagation with static friction μ.

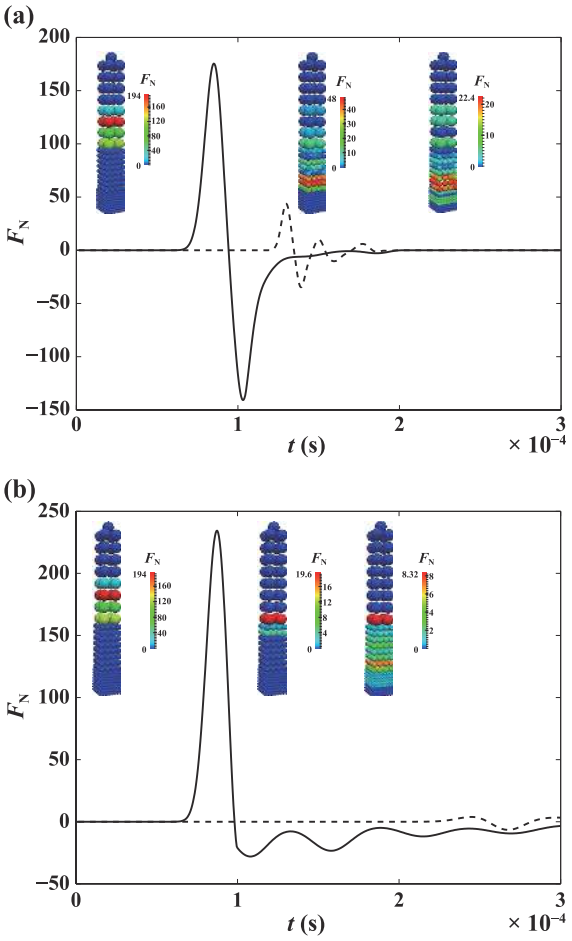

Fig. 8 Force at an interface sphere in a 3-block system for **(a)** all blocks made from steel sphere and **(b)** block with teflon spheres sandwiched between blocks made from steel sphere. The solid line shows the force on interfacial sphere in the top block while the dashed line shows the force on the interfacial sphere in the second block. The inset shows the vertical cross sectional view of the overall force distribution at different time instants. The color bar shows the absolute value of the normal force acting on a sphere.

would be significant. At this moment we concentrate only on the downward propagation of energy.

In **Fig. 8** we show the vertical force propagation in a three block system. Two different systems are considered. In the first, all the blocks are made of steel spheres, while in the second, a block made from lighter mass Teflon spheres is sandwiched between blocks made from heavier steel spheres. In both the systems within the top block the force propagates as a single hump. At the top interface the transmission of force is significantly different. In the first case when the mass mismatch is comparatively smaller the force gets transmitted almost entirely and over a shorter time interval. As mass mismatch increases, the force propagates slowly inside the Teflon block and is more uniformly distributed over the overall length of the block. There is also a sharp reduction of the maximum force on the sphere at the interface in the second arrangement.

4. Conclusions

The wave propagation in the presence of mass mismatch was investigated numerically for an impact decimation system. Our numerical simulations show that such a system is capable of suppressing incident impact significantly. The setup presented here takes advantage of the fact that when a solitary wave crosses from a denser to a lighter medium, a series of solitary waves with smaller energies are generated. This splitting is also borne out of the approximate hard sphere collision theory for the system under consideration. A larger mass difference at the interface results in more splitting and thereby lesser energy in each pulse. A block with smaller mass spheres sandwiched between blocks with heavier mass spheres on both sides shows better impact decimation capability. The

arrangement of spheres at the interface (triangular in 2D and pyramid in 3D) leads to energy being partitioned between more spheres at the interface. The proposed three dimensional system is therefore seen to demonstrate superior impact dispersion capabilities. The sideward propagation is however significantly larger in three dimensions. While we have not considered this situation in the current work, in actual design of systems this would be quite important. Since the impact dispersion and decimation is due to the geometry of the packing at the interface, the qualitative features should not be affected by varying the size or the angle of impact of the striker.

Nomenclature

F_n	normal force (N)
F_t	tangential force (N)
k_n	normal spring constant (N/m)
k_t	tangential spring constant (N/m)
δ_n	normal overlap (m)
δ_t	tangential overlap (m)
μ	static friction
Y	Young's modulus (Pa)
v	Poisson's ratio
R	radius of the sphere (m)
ρ	density of the sphere (kg/m^3)
R^*	effective radius of two particles in contact
Y^*	effective Young's modulus
G	Shear modulus (Pa)

References

Abd-Elhady M.S., Abd-Elhady S., Rindt C.C.M., Van Steenhoven A.A., Force propagation speed in a bed of particles due to an incident particle impact, Adv. Powder Technol., 21 (2010) 150–164.

Awasthi A.P., Smith K.J., Geubelle P.H., Lambros J., Propagation of solitary waves in 2D granular media, Mechanics of Materials, 54 (2012) 100–112.

Awasthi A.P., Wang Z., Broadhurst N., Geubelle P., Impact response of granular layers, Granular Matter, 17 (2015) 27–31.

Burgoyne H.A., Daraio C., Elastic–plastic wave Propagation in uniform and periodic granular chains, Journal of Applied Mechanics, 82(8) (2015) 081002.

Burgoyne H.A., Newman J.A., Jackson W.C., Daraio C., Guided impact mitigation in 2D and 3D granular crystals, Procedia Engineering, 103 (2015) 52–59.

Coste C., Falcon E., Fauve S., Solitary waves in a chain of beads under Hertz contact, Phys. Rev. E, 56 (1997) 6104–6117.

Cundall P.A., Strack O.D.L., A discrete numerical model for granular assemblies, Géotechnique, 29(1) (1979) 47–65.

Daraio C., Nesterenko V.F., Herbold E.B., Jin S., Energy trapping and shock disintegration in composite granular medium, Phys. Rev. Lett., 96 (2006) 058002.

Doney R., Sen S., Impulse absorption by tapered horizontal alignment of elastic spheres, Phys. Rev. E, 72 (2005) 041304.

Doney R., Sen S., Decorated, tapered and highly nonlinear granular chain, Phys. Rev. Lett., 97 (2006) 155502.

Fraternali F., Porter M.A., Daraio C., Optimal design of composite granular protectors, Mech. Adv. Mat. Struct., 17 (2010) 1–19.

Hertz H., Über die Berührung fester elastischer Körper, Journal für die reine und angewandte, Mathematik, 92 (1881) 156–171.

Hong J., Xu A., Effects of gravity and nonlinearity on the waves in the granular chain, Phys. Rev. E, 63 (2001) 061301.

Hong J., Xu A., Nondestructive identification of impurities in granular medium, Appl. Phys. Lett., 81 (2002) 4868–4870.

Hong J., Universal power-law decay of the impulse energy in granular protectors, Phys. Rev. Lett., 97 (2005) 108001.

Jaeger H.M., Nagel S.R., Behringer R.P., Granular solids, liquids, and gases, Rev. Mod. Phys., 68 (1996) 1259.

Job S., Melo F., Sokolow A., Sen S., Solitary wave trains in granular chains: experiments, theory and simulations, Granular Matter, 10 (2007) 13–20.

Katsuragi H., Physics of soft impact and cratering, Springer, Tokyo (2016). ISBN 978-4-431-55648-0.

Kloss C., Goniva C., Hager A., Amberger S., Pirker S., Models, algorithms and validation of opensource DEM and CFD-DEM, Progr.Computat. Fluid Dyn., 12 (2012) 140–152.

Leonard A., Daraio C., Stress wave anisotropy in centered square highly nonlinear granular systems, Phys. Rev. Lett., 108 (2012) 21430.

Leonard A., Fraternali F., Daraio C., Directional wave propagation in a highly nonlinear square packing of spheres, Exp. Mech., 57 (2013) 327–337.

Leonard A., Daraio C., Awasthi A., Geubelle P., Effects of weak disorder on stress-wave anisotropy in centered square nonlinear granular crystals, Phys. Rev. E, 86(3) (2012) 031305.

Leonard A., Chong C., Kevrekidis P.G., Daraio C., Traveling waves in 2D hexagonal granular crystal lattices, Granular Matter, 16 (2014) 531–542.

Lindenberg K., Harbola U., Romero H., Rosas A., Pulse propagation in granular chains, Am. Inst. Phys. Conf. Ser., 1339 (2011) 97–110.

Machado L.P., Rosas A., Lindenberg K., A quasi-unidimensional granular chain to attenuate impact, Eur. Phys. J. E, 37(11) (2014) 1–7.

Mackay R.S., Solitary waves in a chain of beads under Hertz contact, Phys. Lett. A, 251 (1999) 191–192.

Manjunath M., Awasthi A.P., Geubelle P.H., Plane wave propagation in 2D and 3D monodisperse periodic granular media, Granular Matter, 16 (2014) 141–150.

Melo F., Job S., Santibanez F., Tapia F., Experimental evidence

of shock mitigation in a Hertzian tapered chain, Phys. Rev. E, 73 (2006) 041305.

Nakagawa M., Agui J.H., Wu D.T., Extramiana D., Impulse dispersion in a tapered granular chain, Granular Matter, 4 (2003) 167–174.

Nesterenko V.F., Propagation of nonlinear compression pulses in granular media, J. Appl. Mech. Tech. Phys., 24 (1983) 733–743.

Nesterenko V.F., Dynamics of heterogeneous materials, Springer, New York, 2001.

Nesterenko V.F., Daraio C., Herbold E.B., Jin S., Anomalous wave reflection at the interface of two strongly nonlinear granular media, Phys. Rev. Lett., 95 (2005) 158702.

Nishida M., Tanaka K., Kunimochi T., Takagi T., Discrete element simulation in projectile impacts on granular materials, Proc. 23rd Int. Symp. Shock Waves, (2001) 655–661.

Nishida M., Tanaka K., Matsumoto Y., Discrete element method simulation of the restitutive characteristics of a steel spherical projectile from a particulate aggregation, JSME international journal, Series A, Solid mechanics and material engineering, 47(3) (2004) 438–447.

Nishida M., Tanaka Y., DEM simulations and experiments for projectile impacting two-dimensional particle packings including dissimilar material layers, Granular Matter, 12 (2010) 357–368.

Pal R.K., Awasthi A.P., Geubelle P.H., Wave propagation in elasto-plastic granular systems, Granular Matter, 15 (2013) 747–758.

Plimpton S.J., Fast parallel algorithms for short-range molecular dynamics, J. Comput. Phys., 117(1) (1995) 1–19.

Rossmanith H.P., Shukla A., Photoelastic investigation of dynamic load transfer in granular media, Acta Mech., 42 (1982) 211–225.

Sadd M.H., Tai Q., Shukla A., Contact law effects on wave propagation in particulate materials using distinct element modelling, Int. J. Non-linear Mech., 28 (1993) 251–265.

Sen S., Manciu M., Solitary wave dynamics in Generalized Hertz chains: An improved solution to the equation of motion, Phys. Rev. E, 64 (2001) 056605.

Sen S., Hong J., Bang J., Avalos E., Doney R., Solitary waves in the granular chain, Phys. Rept., 462 (2008) 21–66.

Sinkovits R.S., Sen S., Nonlinear dynamics in granular columns, Phys. Rev. Lett., 74 (1995), 2686.

Tanaka K., Nishida M., Kunimochi T., Takagi T., Discrete element simulation and experiment for dynamic response of two-dimensional granular matter to impact of a spherical projectile, Powder Technol., 124 (2002) 160–173.

Tichler A.M., Go'mez L.R., Upadhyaya N., Campman X., Nesterenko V.F., Vitelli V., Transmission and reflection of strongly nonlinear solitary waves at granular interfaces, Phys. Rev. Lett., 111 (2013) 048001.

Tiwari M., Krishna Mohan T.R., Sen S., Decorated granular layers for impact decimation, Granular Matter, 18 (2016) 1–5.

Wang P.J., Xia J.H., Li Y.D., Liu C.S., Crossover in the power-law behavior of confined energy in a composite granular chain, Phys. Rev. E, 74 (2007) 041305.

Zhu Y., Shukla A., Sadd M., The effect of microstructural fabric on dynamic load transfer in two dimensional assemblies of elliptical particles, J. Mech. Phys. Solids, 44 (1996) 1283–1303.

Author's short biography

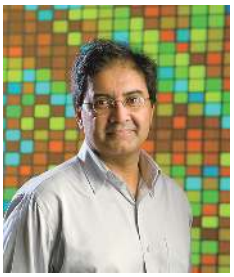

Surajit Sen

Surajit Sen is a Professor of Physics at the State University of New York at Buffalo. His research interests are focused on understanding the dynamics of strongly nonlinear systems. He has worked on impulse propagation in granular systems since 1995. He received his PhD in Physics from the University of Georgia in 1990 and is a Fellow of the American Physical Society and the American Association for the Advancement of Science and serves as an editor of International Journal of Modern Physics B and Modern Physics Letters B.

T. R. Krishna Mohan

Krishna Mohan, T. R. is currently working as a Scientist at CSIR Fourth Paradigm Institute in Bangalore, India where he has been working since 1991. In between, he worked at State University of New York at Buffalo for around four years at the Department of Physics and Department of Pharmaceutics. He received his PhD. from Jawaharlal Nehru University, New Delhi, India in 1988 working on nonlinear dynamics. His current interests include, apart from impulse absorption in granular systems, modelling of CNS, earthquake dynamics and nonlinear dynamics of FPU-like systems.

Mukesh Tiwari

Mukesh Tiwari is currently an Associate Professor at the Dhirbubhai Ambani Institute of Information and Communication Technology (DA-IICT) where he has been working since 2009. He received his M.Sc degree in Physics from Indian Institute of Technology, Delhi in 2003 and PhD in Optical Science and Engineering from the University of New Mexico, USA in 2008. His research interests are mainly focused on statistical physics and nonlinear systems.